Bioconjugate Chemistry

Article

pubs.acs.org/bc

Homing Peptide-Conjugated Gold Nanorods: The Effect of Amino Acid Sequence Display on Nanorod Uptake and Cellular Proliferation

Alaaldin M. Alkilany,[†] Stefano P. Boulos,[‡] Samuel E. Lohse,[‡] Lucas B. Thompson,[§] and Catherine J. Murphy*[,‡]

[†]Department of Pharmaceutics & Pharmaceutical Technology, Faculty of Pharmacy, The University of Jordan, Amman 11942, Jordan

[‡]Department of Chemistry, University of Illinois at Urbana−Champaign, 600 South Mathews Avenue, Urbana, Illinois 61801, United States

[§]Department of Chemistry, Gettysburg College, 300 North Washington Street, Gettysburg, Pennsylvania 17325, United States

ABSTRACT: Gold nanorods (GNRs) have attracted significant interest in the field of medicine as theranostic agents for both imaging and photothermal ablation of cancerous cells/tissues. Targeting theranostic GNRs specifically to cancer cells is necessary to enhance treatment efficacy and minimize undesired side effects. In this study, targeting functionalized GNR to EphA2 receptors that are overexpressed on prostate cancer cells was investigated as a strategy to achieve enhanced GNR uptake by cancer cells. In addition, the influence of targeting peptide orientation on functionalized GNR uptake by PC-3 cells was explored. GNRs of aspect ratio 4 were functionalized with an EphA2 homing peptide, YSA, using a layer-by-layer polypeptide wrapping approach. In parallel, an analogous population of YSA-modified GNRs, which display a reversed YSA peptide, with the N- and C- termini reversed, was also prepared. GC-MS analysis of the YSA-GNRs indicated that functionalized GNRs displayed approximately 3000 peptides/GNR. The functionalized GNRs remained well-dispersed in biological media for short times (<24 h). An increase in GNRs uptake of the YSA-GNRs by PC-3 cells, compared to the reversed YSA-GNRs, was observed under identical incubation conditions. Lastly, the effect of the YSA-GNRs binding to EphA2 receptors on prostate cancer cell proliferation was also studied. The YSA-functionalized GNRs inhibit PC-3 proliferation at a significantly lower effective dose than free YSA. Overall, the polypeptide LBL deposition technique provides a facile route to target nanoparticles to overexpressed cellular receptors, with the caveat that the specific orientation and display of the targeting moiety plays a critical role in the interaction between the nanoparticle and the cell.

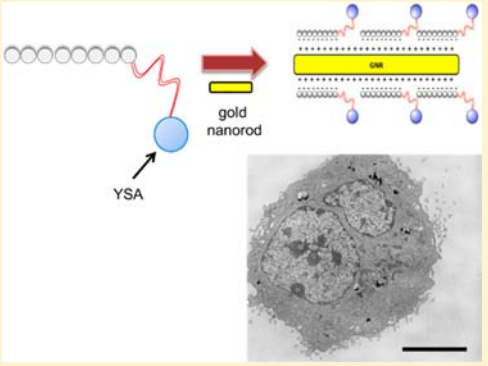

INTRODUCTION

Colloidal nanoparticles functionalized with targeting/therapeutic agents have the potential to revolutionize the diagnosis and treatment of a variety of medical conditions. Gold nanoparticles (GNPs), in particular, are excellent theranostic material candidates (NP that can perform both *thera*peutic and dia*gnostic* functions) because of their optical and photothermal properties.[1−8] GNPs can be synthesized in a variety of sizes and shapes, and are composed of a core metal that is biocompatible (in its bulk form).[1] Furthermore, anisotropic gold nanoparticles such as nanorods (GNRs) exhibit superior optical properties over their spherical counterparts, in particular, improved absorption of near-infrared light.[9,10] GNPs enable biological applications such as tumor imaging, photothermal tumor ablation, and drug delivery.[11−13] The ability to precisely control GNP surface chemistry further increases their functionality, and provides a potential opportunity to target GNPs to specific cells or even organelles in biological systems.[14,15] This provides an opportunity to influence GNR biological transport through rational design of their surface chemistry, potentially including the ability to specifically target cells.

At present, targeted nanoparticles are engineered via surface functionalization with recognition moieties (antibodies,[16] homing peptides,[17] oligonucleotides,[18] aptamers[19]) that are supposed to bind at specific receptors on the surface of particular (usually cancer) cells.[20,21] One particularly appealing target is a class of membrane-bound receptors called Ephrin (Eph) receptors. Eph receptors and the corresponding ephrin ligands (a subclass of receptor tyrosine kinases) are extensively involved in the control of intercellular signaling processes that govern cell division and proliferation.[22,23] These Eph receptors are 10−100× overexpressed in a wide range of cancer cells,[24] making them, in principle, a promising basis for the specific targeting of functionalized NPs to cancer cells. Consequently, the use of ephrin ligands, as well as synthetic analogues of the ligand, has been investigated as a means of targeting cancer cells and potentially inducing apoptosis or reducing metastasis. In 2008, Gobin et al. demonstrated that ephrin-functionalized gold nanoshells could be used to improve nanoshell uptake by

Received: April 19, 2014
Revised: May 15, 2014
Published: May 20, 2014

   dx.doi.org/10.1021/bc500174b | *Bioconjugate Chem.* 2014, 25, 1162−1171

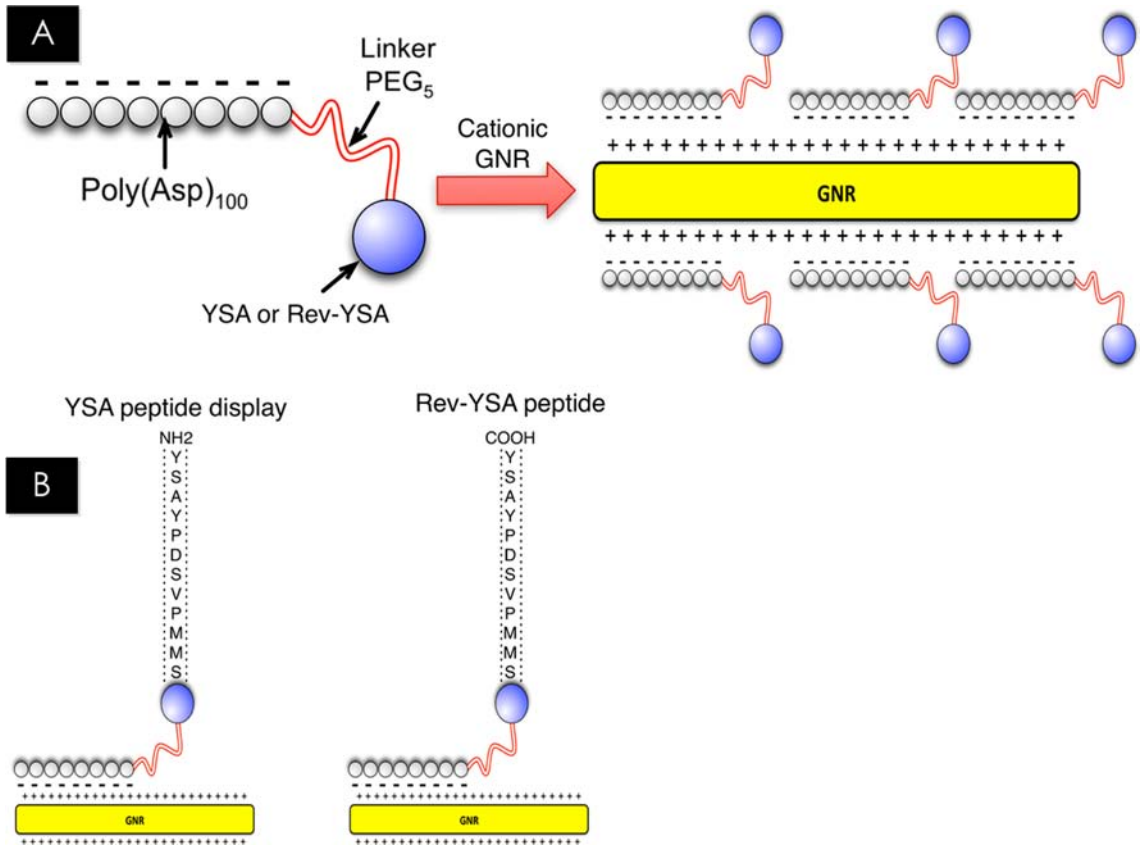

Figure 1. (A) Schematic showing the polyelectrolyte wrapping process at the surface of the cationic CTAB-GNR with the anionic YSA-PEG-poly(Asp) ligand. The ligand contains three specific regions: a polyaspartate region (100 residues) coupled to a PEG linker (5 monomer units) and terminated in the YSA peptide (12 mer). The YSA-PEG-poly(Asp) chain is attached to the surface of the GNR using a layer-by-layer polyelectrolyte procedure. (B) Schematic showing the arrangement of the YSA peptide versus the reversed YSA version (Rev-YSA) to control molecular display at the GNR surface.

prostate cancer cells *in vitro* (compared to poly(ethyelene glycol)-functionalized nanoshells), and consequently enhance photothermal therapy efficiency.[20] More recently, the potential to use ephrin receptor binding as a method for peptide-functionalized nanoparticles to target cancer cells during metastasis and act as enhanced drug delivery vehicles has also been demonstrated.[25]

In this study, we sought to develop a more systematic understanding of how ligand functionalized-GNRs could be used to control the interactions of GNRs with cancer cells that overexpress EphA2 receptors. Specifically, we examined how the orientation of an EphA2-targeting peptide, YSA, at the GNR surface influenced GNR uptake by PC-3 cells and how YSA-functionalized GNR binding to PC-3 cells influenced the rate of PC-3 cellular proliferation. The YSA peptide has previously been deployed *in vitro* as a homing peptide against prostate cancer cells (the PC-3 cultured cell line).[22] This peptide was chosen for its relatively high specificity and binding affinity for EphA2 receptors (K_d = 187 ± 7 nM).[22] The chemical strategy for surface functionalization was a polyelectrolyte layer-by-layer wrapping approach that we have previously described.[26] The YSA peptide (N-YSAYPDSVPMMS-C) was linked to a polyelectrolyte chain (polyaspartate) via a PEG linker, in order to enable polyelectrolyte wrapping around initially cationic GNRs (Figure 1).[25] In order to assess how the molecular display of the peptide on a surface might impact cell–nanoparticle interaction, a version of the YSA peptide with the N- and C-terminus reversed (Rev-YSA) was also linked to a polyaspartate chain via a PEG linker to coat another batch of GNRs (Figure 1). Previous work has shown that the N-terminus of the ligand is critical in ligand–receptor binding compared to the C-terminus.[27−29] Using the YSA-functionalized GNR, we explored how the presence and orientation of the YSA peptide displayed on the GNR surface influences GNR stability in biological media, GNRs cellular uptake, *in vitro* toxicity of GNRs, and cell proliferation in prostate cancer cell cultures.

■ RESULTS AND DISCUSSION

The potential of functionalized GNRs as hybrid nanotherapeutics to bind specifically and influence the growth of PC-3 cancer cells in vitro was investigated. In order to understand how peptide orientation influenced GNR–cellular interactions, YSA-GNR and Rev-YSA-GNR were prepared first by synthesizing the YSA and Rev-YSA peptides, covalently linking them to polyaspartate through the N- or C-terminus with a short PEG spacer chain, and finally wrapping the peptide complexes at cationic GNR surfaces using the previously reported layer-by-layer functionalization procedure (Figure 1).[26] The use of a short PEG linker has been shown to enhance peptide targeting of monoclonal antibodies to their receptors.[30] We aimed to keep constant PEG linker for both YSA and Rev-YSA to eliminate the effect of linker length, which is an important factor and could be the subject of subsequent studies.[30]

dx.doi.org/10.1021/bc500174b | *Bioconjugate Chem.* 2014, 25, 1162−1171

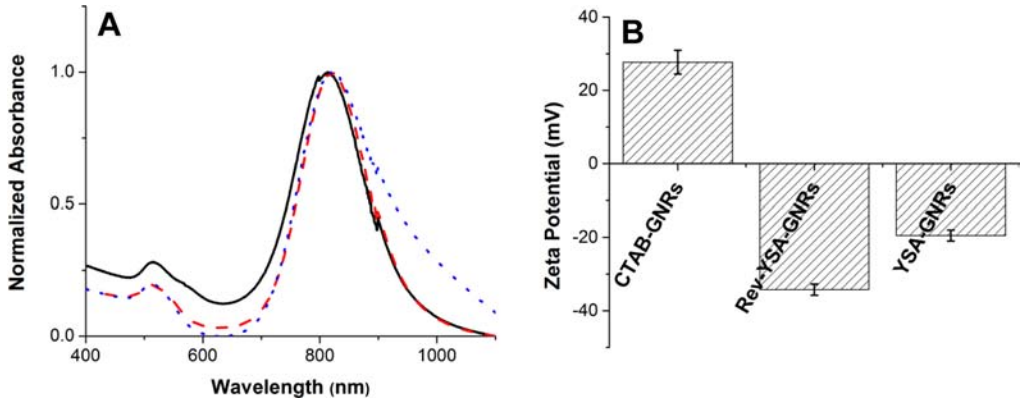

Figure 2. (A) UV−vis absorbance spectra of CTAB-GNR (——), Rev-YSA-GNR (- - -), and YSA-GNR (···) showing minimal peak broadening. (B) Zeta potential measurements for CTAB-GNR, Rev-YSA-GNR, and YSA-GNR. All measurements were carried out in nanopure deionized water.

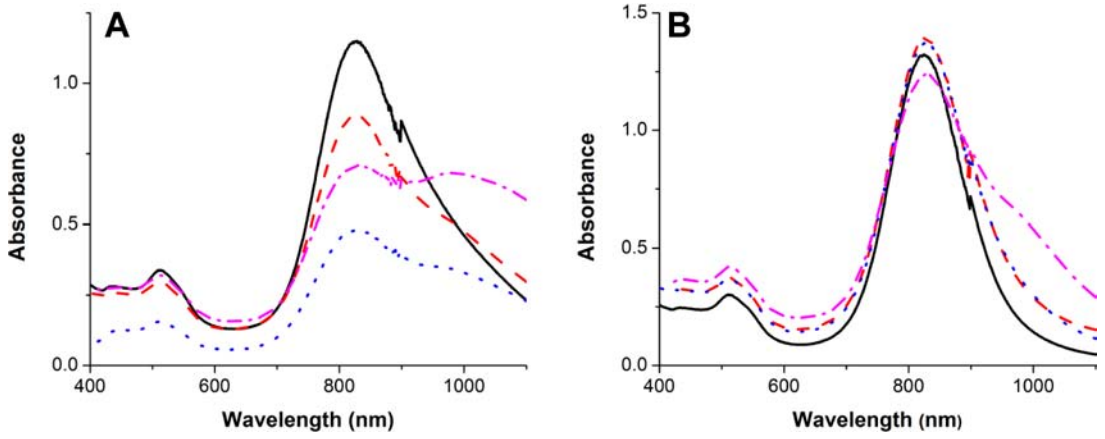

Figure 3. UV−vis spectra showing the absorbance of YSA-GNR (A) and Rev-YSA-GNR (B) incubated at different time points (— 0 h), (- - - 3 h), (··· 6 h), (- · - ·24 h) in PC-3 cell culture media at 37 °C. At t = 0 particles are in water. The formation of an extra peak at about 1000 nm suggests GNR aggregation.

Using these GNR probes, we investigated how the inclusion of the YSA moiety on the GNR surface influenced GNR interactions with prostate cancer cell cultures in which the EphA2 receptor is overexpressed. A series of assays were performed to characterize and probe the efficiency of the YSA-functionalized GNRs as a nanotherapeutic system, including how EphA2 targeting influences GNR uptake, how the presence of the YSA moiety influences GNR toxicity in cancer cells, and how binding of the YSA-GNR to the PC-3 cell surface affects prostate cancer cell proliferation.

UV−vis absorbance measurements of the GNRs were taken before and after functionalization. The initial surface coating of the GNR, the cationic surfactant cetyltrimethylammonium bromide (CTAB), necessitates an anionic wrapping agent; hence, sodium polyaspartate was chosen. The longitudinal plasmon peak of the GNR is highly sensitive to changes in particle environment, and significant broadening of this plasmon peak is expected when aggregation occurs.[31,32] From the UV−vis measurements (Figure 2A), limited peak broadening is observed; thus, minimal aggregation occurs after polyelectrolyte wrapping in the presence of either version of the peptide. We also monitored the change in overall surface charge of the GNR by taking ζ-potential measurements before and after the layer-by-layer coating. Since both versions of the peptide are covalently linked to a negatively charged poly(aspartate) chain, a reverse in overall surface charge is expected. A change from ∼+30 mV for CTAB-GNR to −20 mV and −30 mV for YSA- and Rev-YSA-GNR, respectively, is observed (Figure 2B). These results confirm the presence of both YSA- and Rev-YSA-polyelectrolytes at the GNR surface. The less negative zeta potential observed for YSA-GNR is most likely due to the free terminal amine groups which would be cationic at neutral pH; for Rev-YSA-GNR, the free C-terminal implies terminal carboxylic acid groups which would be anionic at neutral pH. We note that deposition of polyelectrolytes onto the surface of charged gold nanoparticles is reported to be irreversible, resulting in a stable coating with very low tendency of desorption from the surface.[33,34]

Quantification of the number of peptides per GNR was performed using gas chromatography coupled with mass spectrometry (GC-MS). In order to determine the number of bound peptides, the supernatant from the polyelectrolyte coating reaction was collected following centrifugation. The concentration of free peptide remaining in the supernatant was quantified by GC-MS following peptide digestion using acid hydrolysis. By subtracting the amount of aspartic acid detected in supernatants from the amount detected in control solutions (at the same initial concentration of the wrapping reaction, but with no GNR), the amount of peptide bound per GNR was calculated. The amount of YSA-polyelectrolyte and Rev-YSA-polyelectrolyte bound to the GNR was found to be 38.8 ± 7.2 μg/mL and 27.3 ± 4.8 μg/mL, respectively. This corresponds

dx.doi.org/10.1021/bc500174b | Bioconjugate Chem. 2014, 25, 1162−1171

to 4370 ± 810 and 3070 ± 540 peptides/GNR, respectively, for the YSA and Rev-YSA functionalization.

Assuming an average dimension of 64 × 14 nm^2 for each GNR, the surface area of the GNR is approximately 3100 nm^2 per particle. We estimate that a single YSA-PEG-Poly(Asp) peptide would occupy 22 nm^2 if stretched out to make maximum contact with the surface. Therefore, the minimal monolayer loading we would expect is ∼140 peptides/GNR. Since the GC-MS analysis indicates several thousand ligands are present per GNR, either (i) there is still free peptide present that we were unable to purify away, (ii) multilayers of peptides are present, or (iii) there is a peptide monolayer, but they are anchored to the surface so that they either wrap the nanorod well or point primarily vertically into the solution. In this case, the peptide footprint may be much smaller. Assuming a 1 nm^2 peptide footprint, a monolayer of peptide could provide several thousand peptides per GNR.

The precise characterization of GNR physiochemical properties in cell media is essential to accurately understand how their surface chemistry influences their interaction with cell cultures in vitro. Prior to incubating the YSA- and Rev-YSA-GNRs with PC-3 cells, we investigated their stability in PC-3 cell media over an extended period of time by monitoring changes in their absorbance spectra (Figure 3). Results confirmed that the functionalized GNRs remained well-dispersed in the media after several hours of incubation. However, over time, the formation of a third peak around 1000 nm can be seen, suggesting the formation of particle aggregates at longer incubation times. For the YSA-GNRs, this peak is first observed after 3 h of incubation time, while in the Rev-YSA-GNR solution, significant aggregation is not observed until nearly 24 h. Functionalized nanoparticles often aggregate over time in cellular media, a process which likely results from a competition between ion-induced GNP aggregation and GNP coating by serum proteins.[9,35] However, all subsequent uptake experiments for YSA-GNR and Rev-YSA-GNR were performed at an incubation time of t = 2 h, a time point corresponding to minimal GNR aggregation for both types of nanoparticles. The differential colloidal stability of YSA-GNRs and Rev-YSA-GNRs could be attributed to the reversal of the N- and C-termini, which changes the effective surface charge as discussed earlier.

The uptake of both YSA-GNRs and Rev-YSA-GNRs in vitro was studied in order to probe the specificity of YSA-GNR for EphA2 receptors. Following YSA binding to the Ephrin A2 receptor, the bound ligand−receptor complex can be taken up into the cell via endocytosis.[22−24] Therefore, both GNRs bound to the cell surface and GNRs that have been internalized by the cell may indicate interactions between the YSA-GNRs and the EPhA2 receptors. Inductively coupled plasma mass spectrometry (ICP-MS) was used to detect Au atoms associated with the cancer cells after dosing with GNRs and purifying away excess GNRs. As discussed in the Experimental Procedures (vide infra), while the cells were thoroughly rinsed with buffer to remove loosely adsorbed GNRs, no specific attempt was made to differentiate between GNRs bound to Eph receptors on the cell surface versus GNRs that have been internalized. Therefore, we consider both GNRs that are tightly bound to the cell surface, as well as internalized GNRs, to be "taken up" by the cells in this study. The amount of Au atoms detected was converted to the amount of GNRs based on the volume of a gold nanorod with dimensions of 64 × 14 nm^2. Results showed that YSA-GNRs were taken up by PC-3 cells 60−470% more than Rev-YSA-GNRs, depending on dose, suggesting that the specific interaction of the YSA-functionalized GNR to the EphA2 receptors at the surface of the PC-3 cells does occur, and that molecule display does matter (Table 1). As an additional control, functionalized GNR uptake in a cell line which does not overexpress Eph receptors (human dermal fibroblast cells, HDF) was also investigated.[20] Indeed, we found the amount of targeted GNR associated with HDF cells to be about half of the amount associated with PC-3 cells (Table 1), an encouraging trend, but not the 10−100-fold loss that might be expected based on the cell surface expression difference. Interestingly, both cell lines take up the YSA-GNR more abundantly compare to the reversed version (Rev-YSA-GNR). This observation is understandable if it is considered that EphrinA2 receptors, even though less abundant, are still present in HDF cells,[29] and therefore, the affinity of YSA-GNR for the cell surface will be higher than that of the incorrectly displayed peptide.

Table 1. Quantification of GNR Uptake by PC-3 and HDF Cells via ICP-MS[a]

cell line; initial GNR concentration in particles	YSA-GNR/cell	Rev-YSA-GNR/cell
PC-3 cells; [GNR] = 0.01 nM	10 500 ± 2980	6340 ± 1250
PC-3 cells; [GNR] = 0.05 nM	54 900 ± 8900	11 500 ± 383
HDF cells; [GNR] = 0.05 nM	28 100 ± 2020	5200 ± 1100

[a]Concentrations correspond to those of initial YSA-conjugated GNR and reversed YSA-GNR (per particle) for ∼400 000 cells/mL of cells after 2 h of incubation. Error bars represent standard deviation values of three independent experiments.

We should point out that the targeting specificity of YSA on GNRs is certainly not an all-or-nothing event. Many YSA-GNRs do end up in HDF cells, and many Rev-YSA-GNRs, even with the incorrectly displayed peptide, do end up in PC-3 cells. Thus, we expect that the most useful targeting experiments in nanomedicine ought to focus on finding more specific biological targets; secondarily, molecular display ought to be considered and controlled.

We also studied the viability of PC-3 cells when dosed with different concentration of both YSA- and Rev-YSA-GNRs using the MTS assay.[36] We found that the cells were viable after being incubated for a period of 2 h with both GNRs. Both YSA-GNR and Rev-YSA-GNR concentrations of 0.01−0.1 nM in particles did not alter the viability of the PC-3 cells (same concentration range used in the GNR uptake studies) (Figure 4). Consequently, we found that both classes of functionalized GNRs induced no acute cytotoxicity under the concentrations tested. Furthermore, the in vitro biocompatibility of the functionalized GNRs suggests that the cytotoxic CTAB retained in the layer below the peptide coating is not released from the GNR surface in sufficient quantities to promote significant cell death.

It has been suggested that the binding of the natural targeting ligand, ephrinA1, to EphA2 cell surface receptors leads to receptor phosphorylation and down-regulation of cell proliferation.[23] Activated EphA2 receptors thus launch signaling events that lead to inhibition and reversal of malignant traits in the cell such as proliferation and invasiveness.[37] However, in pathologic tissues the EphA2 receptor is up-regulated, and the lack of ligand to bind and activate those receptors leads to cell proliferation, tumor metastasis, and ultimately poor prognosis.[24] It has been shown that the YSA peptide functions

dx.doi.org/10.1021/bc500174b | Bioconjugate Chem. 2014, 25, 1162−1171

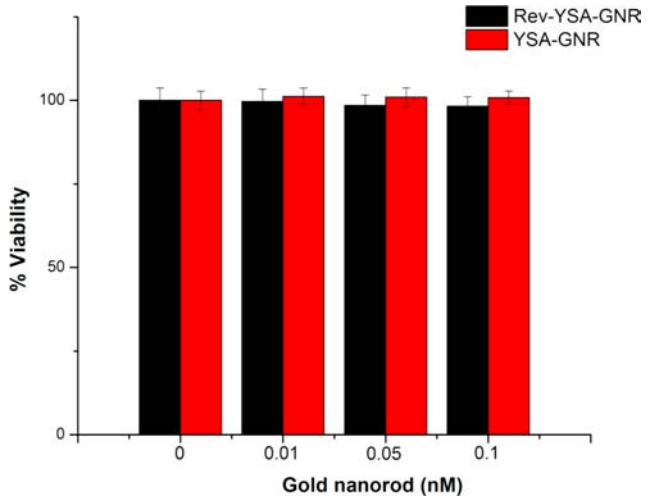

Figure 4. Cellular viability results of PC-3 cells exposed to YSA-GNRs and Rev-YSA-GNRs at sub-lethal concentrations using the MTS assay after t = 2 h. Error bars represent standard deviation values of three independent experiments.

similarly to the ephrinA1 ligand.[22] Therefore, we studied the effect of the binding of the YSA peptide, both free and bound to GNRs, on the proliferation of PC-3 cells for defined dosages (Figure 5), in order to determine whether the functionalized GNR could potentially act as a therapeutic to influence the rate of cancer cell proliferation.

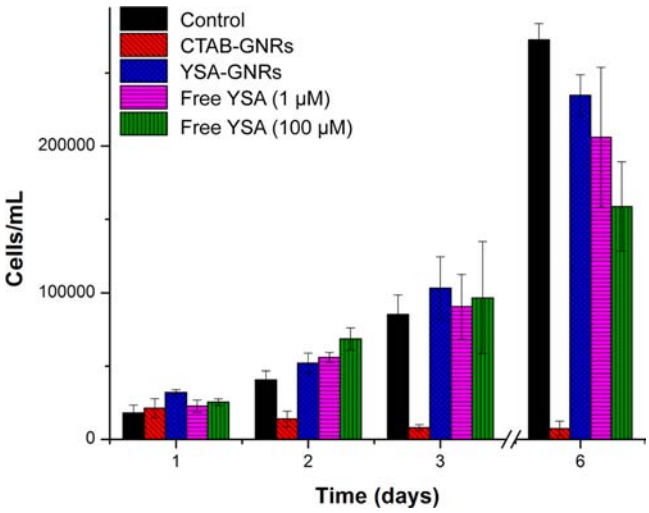

Figure 5. Proliferation of PC-3 cells in culture media free of GNR (black), culture media with 0.1 nM CTAB-GNR (red), culture media with 0.1 nM YSA-GNR (blue), culture media with 1 μM free YSA (pink), and culture media with 100 μM free YSA (green). Error bars represent standard deviation values of three independent experiments.

In order to determine the influence of GNR binding on cell proliferation, unfunctionalized GNRs (CTAB-GNRs), YSA-GNRs, and free YSA ligand were added to PC-3 cell cultures and incubated over a period of 6 days. Cells in which the culture media was free of GNRs were used as controls. Cells were counted at day 1, 2, 3, and 6. The CTAB-GNRs decreased the proliferation of PC-3 cells (Figure 5), probably due to the toxicity of desorbed CTAB at submicromolar concentrations, as we have reported before if the CTAB on GNRs is not encapsulated in a polymeric thin film.[38] PC-3 cells in the presence of YSA-GNRs showed a slight decrease in cell proliferation, for an exposure that is effectively ~440 nM in YSA (assuming ~4400 peptides bound per GNR, for 0.1 nM YSA-GNR particle concentrations). For comparison, the effect of free YSA versus YSA-GNR was also studied. PC-3 cells were incubated with free YSA (1 and 100 μM) and the rates of proliferation of the cells were monitored. As for the YSA-GNRs, no significant difference was observed over a 3-day period; however, after 6 days of incubation, the proliferation rate decreased significantly in the presence of free YSA at a high concentration of 100 μM. Interestingly, the YSA-GNRs have no significant impact on cell proliferation until long after binding and cellular uptake of YSA-GNRs have occurred. Furthermore, since the YSA-GNRs aggregate in the cell media within 6 h, it appears that YSA-GNR aggregates may be playing a role in reducing the rate of cell proliferation. This is a potentially important observation, as many functionalized NPs aggregate rapidly in cell media, and considering that the influence of NP aggregates on cell behavior in vitro is essential to accurately predict the behavior of functionalized nanomaterials at the bionano interface.

In comparing YSA-GNR to free YSA (Figure 5), it is evident that the degree of cell proliferation is statistically insignificant between 1 μM YSA and 0.1 nM YSA-GNR. Considering that there are ~4400 YSA peptides per GNR, the effective YSA concentration in the YSA-GNR samples could be as high 0.44 μM. However, it should be noted that since the exact orientation and display of the YSA peptides on the GNR surface is difficult to unambiguously characterize, the actual number of YSA peptides displayed by the GNR that are bioavailable may be quite a bit lower. Nevertheless, this opens the possibility that by putting YSA on a nanoparticle surface, the effective dose can be lowered by a factor of 2−3 on a per molecule basis. Dreaden et al. showed that tamoxifen-poly(ethylene glycol)-thiol gold nanoparticle conjugates bind estrogen receptors with up to 2.7-fold enhanced drug potency in vitro compared to free tamoxifen molecules.[39] Our results confirm the concept of lowering doses to cells by multivalent attachment of small molecules on nanoparticles.[39−42]

To evaluate the contribution of ligand−receptor binding to the overall cellular uptake, we undertook a competition experiment between free YSA and YSA-GNR. A solution containing a mixture of YSA-GNR (0.1 nM) and free YSA peptide at high concentration (1 mM) was used to dose PC-3 cells for a period of 2 h in either cell media or PBS buffer, and GNR uptake was analyzed in both cell media and buffer. In an ideal system we expect the free YSA peptide to bind to the EphA2 receptors at a much higher rate compared to the YSA-GNR due to the higher concentration of free YSA present. Thus, EphA2 receptors at the surface of the cells should be blocked and the YSA-GNR binding to these receptors should be limited, which would lead to a decrease in uptake of the functionalized GNR. However, when PC-3 cells were dosed and the GNRs digested into Au atoms for ICP-MS analysis, the amount of GNR taken up by PC-3 cells was found to be at similar level for both solution containing YSA-GNR plus free YSA and YSA-GNR only (Table 2). These results suggest that the free YSA did not affect the uptake of the YSA-GNR within the cells. One explanation for this might be that the binding of YSA-GNR is stronger to the cell surface compared to the free YSA ligand and can bind these receptors with a higher binding constant due to the presence of many YSA copies on the nanoparticle surface (multivalent synergism). However, we

dx.doi.org/10.1021/bc500174b | Bioconjugate Chem. 2014, 25, 1162−1171

Table 2. Quantification of YSA-GNR Uptake by PC-3 via ICP-MS in the Presence and Absence of Free YSA[a]

treatment	in media (GNR/cell)
YSA-GNR + free YSA	$(1.46 \pm 0.1) \times 10^5$
YSA-GNR	$(1.33 \pm 0.2) \times 10^5$

[a]Uptake study was performed with ~30 000 cells/mL of cells after 2 h of incubation. Error bars represent standard deviation values of three independent experiments.

cannot exclude the possibility that the uptake pathway is different for free ligands and ligands that are bound on nanoparticles. It has been previously shown that GNRs free of homing peptide are still taken up by cells arising from cellular recognition of adsorbed proteins from the cellular media via receptor-mediated endocytosis[38] or by receptor-independent uptake mechanisms such as pinocytosis or phagocytosis.[43]

Bio-TEM analysis, which involves electron imaging of fixed PC-3 cells previously incubated with GNRs, shows YSA-GNRs and Rev-YSA-GNRs inside the cells (Figure 6). PC-3 cells were dosed with both YSA-GNR and Rev-YSA-GNR at a final concentration of 0.1 nM. Cells were then washed, trypsinized, and redispersed in fixative at two different incubation times (2 and 24 h). Bio-TEM imaging revealed that the functionalized GNRs are taken up into the PC-3 cells in a perinuclear fashion trapped in vacuoles. Vacuoles were on average ~0.5 μm in diameter dependent on the number of GNRs entrapped. About 20−60 YSA-GNRs per vacuole after a 2 h incubation period and about 200−500 YSA-GNRs per vacuole after a 24 h period were observed. For Rev-YSA-GNRs about 10−20 GNRs per vacuole were observed after a 2 h period and 50−100 GNR per vacuole after a 24 h period. On average, about 10−20 vacuoles were examined per TEM images. It should also be noted that no membrane-bound GNRs were observed in the bio-TEM images, indicating that the majority of GNRs are actually internalized by the PC-3 cells. From the Bio-TEM results it is evident that YSA-GNRs were more abundant in the cells compared to the reversed version. However, there is no sign of different localization within the cells between the two versions of the functionalized GNR. Cells perceive the nanomaterial, possibly due to their large size, as a foreign object and as a protection mechanism entrap GNRs into vacuoles preventing them from reaching the nucleus. We did not observe a change of GNR localization with a longer period of incubation (24 h), only an increase in uptake of GNRs.

CONCLUSION

Using gold nanorods functionalized with YSA homing peptides, we have shown that YSA-GNR (correct display) associate with PC-3 cells significantly more than Rev-YSA-GNR (incorrectly displaced version control), suggesting that molecule display does matter. A significant difference in the cellular uptake and cell proliferation was observed for YSA-GNR and Rev-YSA-GNR as evident from ICP-MS and TEM analysis for quantitative and qualitative measurements. However, the targeting specificity of YSA on GNR is certainly not an all-or-nothing event. Both YSA-GNR and Rev-YSA-GNR were detected inside cancer cells with significantly different levels. Using a reversed version of homing peptides in combination with the use of gold nanoparticle carriers that allow precise quantification of uptake and visualization of nanoparticles inside cells can be considered a powerful tool to evaluate the specificity of recognition ligands for developing targeted drug delivery systems.

EXPERIMENTAL PROCEDURES

Materials. Chloroauric acid ($HAuCl_4 \cdot 3H_2O$, 99.9%), sodium borohydride ($NaBH_4$, 99%), silver nitrate ($AgNO_3$, 99+%), cetyltrimethylammonium bromide (CTAB, 99%, Sigma Ultra), sodium chloride, and ascorbic acid (99+%) were obtained from Sigma-Aldrich and used as received. Phosphate buffered saline (PBS, 10×) was purchased from Lonza. The

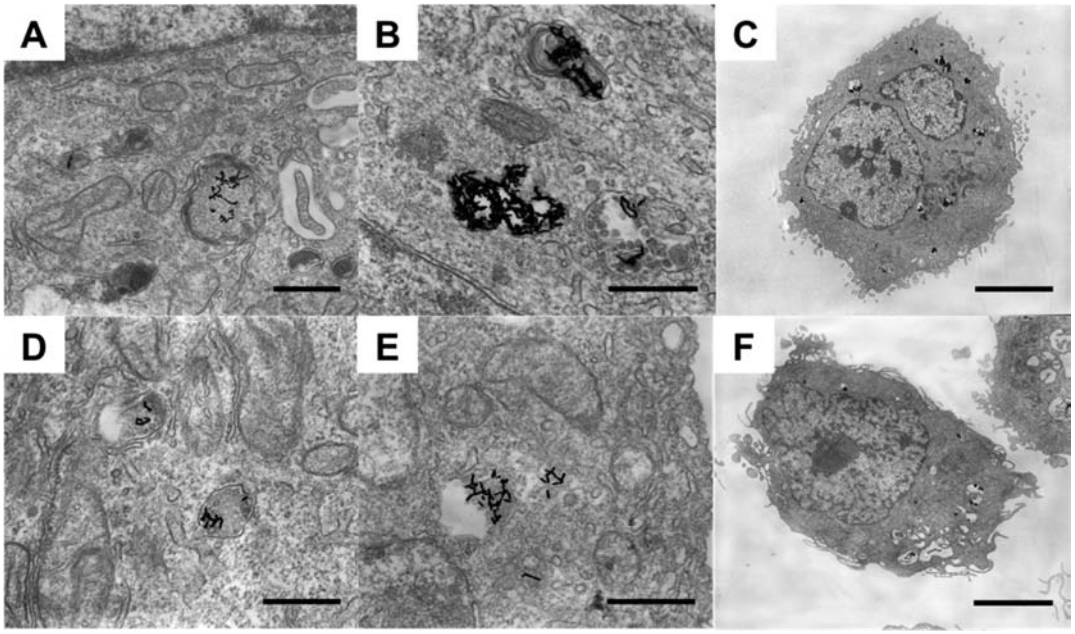

Figure 6. Transmission electron micrographs of PC-3 cells. PC-3 cells (50 000 cells/mL) incubated with YSA-GNR at a concentration of 0.1 nM at t = 2 h (A) and t = 24 h (B and C). PC-3 cells incubated with 0.1 nM Rev-YSA-GNR at t = 2 h (D) and t = 24 h (E and F). Scale bar: A = 1 μm; B, D, and E = 0.5 μm; C and F = 5 μm.

dx.doi.org/10.1021/bc500174b | Bioconjugate Chem. 2014, 25, 1162−1171

MTS assay solution was purchased from Promega. Dialysis cassettes (20K MWCO) were purchased from Thermo Scientific. All GNP solutions were prepared with 18 M.Ω deionized water. All glassware used for GNP was cleaned with *aqua regia* and rinsed thoroughly with deionized water. PC-3 and HDF cell lines were purchased from ATCC. DMEM cellular media supplemented with 4 mM L-glutamine, 1% streptomycin, 1% penicillin, and 10% fetal bovine serum (FBS); and Ham's F12K media supplemented with 4 mM L-glutamine, 1% streptomycin, 1% penicillin, and 10% fetal bovine serum (FBS) were prepared by the Cell Media Facility at the University of Illinois at Urbana−Champaign. The peptides were synthesized by the Carver Biotechnology Center Protein Sciences Facility at the University of Illinois at Urbana−Champaign using a CEM Liberty microwave synthesizer. Fmoc amino acids were obtained from NovaBiochem and HOBt/HBTU activation chemistry was employed for peptide synthesis. The appropriate PEG linker was added to the synthesized peptide on resin, using Fmoc-PEG-COOH (NovaBiochem) and standard HOBt/HBTU chemistry. For N-terminal linking, the PEG was added directly to the N-terminus of the YSA. For C-terminal linking, the linkage was through an orthogonally protected lysine side chain that was incorporated as the first amino acid. Fmoc-HNA (Solulink) was then added using standard HOBt/HBTU chemistry. The modified peptide was then deprotected and cleaved from the resin in the presence of acetone in order to protect the active amine on the HyNic molecule. The polyaspartic acid peptide (Alamanda Polymers) was reacted with S-4FB (Solulink) at 5-fold molar excess according to the manufacturer's recommendations in order to modify the N-terminus of the polyaspartic acid peptide. The modified polyaspartic acid peptide was then dialyzed into conjugation buffer (100 mM Na_3PO_4 pH 6.0, 150 mM NaCl). The modified polyaspartic acid peptide and the modified PEG-peptide (3-fold molar excess) were then mixed in the presence of 10 mM aniline and allowed to react overnight. The conjugated peptides were dialyzed extensively against water and lyophilized.

Instrumentation. Absorption spectra of GNRs were taken on a Cary 500 scan UV−vis-NIR spectrophotometer. ζ-Potential measurements were performed on a Brookhaven Zeta PALS instrument. Absorbance measurements for the MTS were taken on a Spectramax Plus 384 plate reader from Molecular Devices. GC-MS analysis was performed using an Agilent 6890 gas chromatograph equipped with an Agilent 5973 mass selective detector. TEM images were taken using a Hitachi H600 microscope at 75 kV. ICP-MS analysis was performed with a PerkinElmer Elan DRC-e instrument.

Gold Nanorod Synthesis. Anisotropic gold nanoparticles were prepared using a silver nitrate-assisted seeded growth method in the presence of the surface capping agent cetyltrimethylammonium bromide (CTAB), as previously described.[10,26] 1.5 nm CTAB-stabilized gold spheres (seed particles) were first prepared by sodium borohydride reduction. A solution of 2.5×10^{-4} M $HAuCl_4$ was prepared in 0.1 M aqueous CTAB in 50 mL centrifuge tube. $NaBH_4$ (600 μL, of a 10 mM stock solution) was added to the gold/CTAB solution (10 mL) with vigorous stirring for 10 min. The resulting seed particles were then added to a freshly prepared growth solution in order to synthesize gold nanorods of aspect ratio (A.R.) 4. To prepare the gold nanorod growth solution, the following reagents were added (in the order described) to an *aqua regia*-cleaned Erlenmeyer flask: CTAB solution (95 mL of a 0.1 M stock solution), silver nitrate solution (1 mL of a 10 mM stock solution), and $HAuCl_4$ (5 mL of a 10 mM stock solution). An aqueous solution of ascorbic acid (0.55 mL of a 0.1 M stock solution) was then added with gentle mixing. Finally, the gold seed solution (0.12 mL) was added and mixed. The resulting pale brown solution was left undisturbed overnight. The GNR solution was purified twice by centrifugation at 8000 rpm for 30 min to remove excess CTAB. The method yielded GNR of length 64.8 ± 1.7 nm and width 14.8 ± 2.1 nm.

Gold Nanorod Functionalization with YSA-PEG-Poly(Asp) and Rev-YSA-PEG-Poly(Asp). YSA-PEG_5-$Poly(Asp)_{100}$ and Rev-YSA-PEG_5-$Poly(Asp)_{100}$ were coated to the surface of the synthesized CTAB-GNRs using our previously described polyelectrolyte layer-by-layer wrapping method.[26] To functionalize the GNRs, 0.6 mL of 5 mg/mL of the appropriate polyelectrolyte was added to 3 mL CTAB-GNR, along with 0.3 mL of 10 mM NaCl. Solutions were incubated for 12 h at 4 °C. The surface-wrapped GNRs were purified by centrifugation and washing at 5500 RCF for 30 min. Samples were then dialyzed for 24 h in 20K MWCO dialysis cassettes. UV−vis absorbance and ζ-potential measurements were used to characterize the functionalization process; UV−vis spectroscopy was used to determine particle concentration, using previously described methods.[44]

Quantification of Peptide per GNR Obtained by GC-MS. To quantify the amount of peptide adsorbed to the gold nanorod surface, the concentration of aspartate remaining in the supernatants was determined by subtraction (i.e., the bound peptide was determined by subtracting the free peptide from the total peptide). Briefly, CTAB-GNRs were coated with YSA- and Rev-YSA-polyelectrolytes, respectively, as described in the previous section. Free peptide controls were also prepared, by adding 0.6 mL of 5 mg/mL peptide solution to 3.3 mL of a 1.0 mM NaCl. After polyelectrolyte wrapping of the GNR, the supernatants containing the remaining free peptide were collected after repeated centrifugation (3×) at 14 000 rpm for 10 min. This repeated process ensured that the supernatant was free of GNRs. Acid hydrolysis was used to digest free peptide present in the supernatant into its monomeric units.[45] This was done by mixing 0.2 mL of the supernatant or control with 0.8 mL of deionized water and 1 mL of 12 M HCl. The resulting solutions were heated for 36 h at 120 °C. Finally, 200 μL of each sample and each control sample were dried using a centrifugal evaporator. 10 μL of the internal standard (L-*p*-chlorophenylalanine, Science Lab.com, Inc., Houston, TX, USA; 1 mg/mL) was added to each extract and the samples were dried again. 100 μL of water, 100 μL of ethanol/pyridine (4:1), and 50 μL of ethyl chloroformate (ECF) (Aldrich, USA) were added to each dried sample, and the mixture was vortexed for 3−5 s.[46,47] After 20 min, 150 μL of dichloromethane and NaCl (ca. 10 mg) were added and samples were thoroughly shaken for extraction. This upper phase was subjected to GC-MS analysis. The obtained ethoxycarbonyl-ethyl esters were analyzed on Agilent 6890 gas chromatograph equipped with an Agilent 5973 mass selective detector (Agilent Inc., Palo Alto, CA). 5 μL aliquots of sample were injected in a splitless mode, and analyzed on a 15 m Zebron ZB-FFAP column with 0.25 mm I.D. and 0.25 mm film thickness (Phenomenex, Torrance, CA). The injection port and interface temperature were set at 250 °C, and the ion source was set to 230 °C. The helium carrier gas was set at a constant flow rate of 1.6 mL min^{-1}. The oven temperature program was as follows: 5 min isothermal heating at 100 °C, increase at the rate of 10 °C min^{-1} to 260 °C

for the final 9 min. The mass spectrometer was operated in positive electron impact mode (EI) at 69.9 eV ionization energy with an m/z 50−800 scan range. The spectra of all chromatogram peaks were evaluated using the HP Chemstation (Agilent, Palo Alto, CA, USA) and AMDIS (NIST, Gaithersburg, MD, USA) programs. Identification and quantification were performed using the mass spectra obtained from the authentic standards and additionally confirmed with NIST08 and/or W8N08 libraries (John Wiley & Sons, Inc., USA). To allow comparison between samples, all data were normalized to the internal standard (L-*p*-chlorophenylalanine). Calibration curves were generated with concentrations of 100, 75, 50, 20, 10, 5, 2, 1, and 0.5 μg mL^{-1} for each target compound.

Peptide-Functionalized GNR Stability in Cell Media. In order to test the GNR stability in PC-3 cell media, a small aliquot (100 μL) of the functionalized GNR solution was added to 900 μL of the cell media and incubated at 37 °C. UV−vis absorbance measurements of the GNRs in cell media were taken at specific time points from 0 to 24 h. These spectra were analyzed to determine the extent of GNR aggregation over time in the cell media.

Cell Culture Growth and Maintenance. For this project, prostatic adenocarcinoma adult human cells (PC-3), along with human dermal fibroblast cells (HDF), were chosen. PC-3 cells overexpress the ephrinA2 receptor but HDF cells do not. HDF cells were grown in DMEM supplemented with 4 mM L-glutamine, 1% streptomycin, 1% penicillin, and 10% fetal bovine serum (FBS). PC-3 cells were grown in Ham's F12K media supplemented with 4 mM L-glutamine, 1% streptomycin, 1% penicillin, and 10% fetal bovine serum (FBS). Cells were detached from culture with trypsin (0.05%) and EDTA (0.02%) and resuspended in proper media for passaging in wells, flasks, or slides. A hemocytometer was used for cell counting.

PC-3/HDF Cells Dosing with Peptide Functionalized GNR. Both PC-3 and HDF cells were plated in 75 cm^2 rectangular canted neck cell culture flasks with vented caps and allowed to reach ∼80% confluency. Cell cultures were dosed with both YSA-GNRs and Rev-YSA-GNRs at two different concentrations (0.1 and 0.5 nM). Cells were incubated with the GNR for 2 h. After incubation, cells were washed with PBS buffer (2×), split using 0.25% trypsin, and collected by centrifugation. The collected pellet of cells was redispersed in 5 mL of media and the cell clumps were broken down using suction to cause an up and down movement of the liquid with a 10 mL pipet tip. The homogeneous solution was then diluted to 15 mL with media to prepare Solution A. 5 mL of Solution A was further diluted to a volume of 15 mL {Solution B (∼30 000 cells/mL)} and used to plate the PC-3/HDF cells in a 6 well plate for ICP-MS analysis. To do this, 1 mL of the Solution B was added to each well plus 1 mL of fresh media making a final volume of 2 mL. This results in a cell density of ∼15 000 cells/mL. Then, another 5 mL of Solution A was diluted to 30 mL to make Solution C, used for the cytotoxicity study. For the cytotoxicity study, 200 μL of Solution C was added to each well of a 96 well plate. Finally, the last 5 mL of Solution A was diluted to 12 mL and plated into a new cell culture flask for later use.

Cytotoxicity Study in the Presence of YSA- and Rev-YSA-GNRs. We used the MTS assay to determine the viability of cells after incubation with GNRs and also other components that might be present in the nanorod solution. This technique is a colorimetric assay for monitoring the mitochondrial activity of cells.[36] The assay was carried in a 96-well plate and the absorbance at 490 nm, with dimethyl sulfoxide as the solubilization solution, was measured to quantify the amount of dye reduction that occurs, which is directly related to cell mitochondrial activity.

Quantitation of GNR Uptake by ICP-MS. We used inductively coupled plasma mass spectrometry (ICP-MS) to quantify the uptake of GNRs into PC-3 cells. Following incubation at 37 °C, cells were thoroughly washed with PBS buffer to remove excess particles, treated with trypsin, and redispersed in 1 mL of buffer. It should be noted that, while the cells were thoroughly washed with buffer after exposure to functionalized GNRs, no specific etching treatment was used to remove GNRs that were bound to the cell surface versus cells that had actually been internalized by the cells. Therefore, for the purposes of this study, we consider both GNRs that are tightly bound to the cell surface, as well as cells that have been internalized, to have been "taken up" by the cells. We used a hemocytometer to count the number of cells, and then sonicated the solutions for 2 h to completely dissolve the cell membranes. Gold nanorods (associated with cells) were dissolved using 0.4 mL of *aqua regia* (3:1, HCl:HNO_3) for a period of 2 h. The solution was then diluted to 5 mL with deionized water. The samples were then analyzed by ICP-MS (vide supra) to quantify the number of GNRs taken up by the cells (including GNRs closely associated with the cell membranes).

Proliferation Assay of PC-3 Cells. We studied the proliferation of PC-3 cells in the presence of YSA-GNRs, free YSA, and CTAB-GNRs. Cells were plated in 24-well plates at a density of 20 000 cells/mL. After 24 h of incubation time, cells were dosed respectively with YSA-GNR (0.1 nM), CTAB-GNR (0.1 nM), free YSA (1 and 100 μM), and media (control). Proliferation was measured over a period of 6 days by counting the number of cells in each well at the specific time points. The GNR solutions and the free YSA were added only once to the cell cultures, and remained in the cell media throughout the course of the six day experiment.

Competitive Uptake Studies: Free YSA versus YSA-GNR. PC-3 cells were plated and exposed to a solution containing free YSA peptide in excess (1 mM) and YSA-GNR (0.1 nM). The extent of GNR cellular uptake was compared to YSA-GNR uptake from a control solution with only YSA-GNR (0.1 nM). After 2 h of incubation, the media above the PC-3 cells was removed, and the cells were washed twice with PBS buffer. The extent of YSA-GNR uptake in both the presence and the absence of free peptide was then determined by ICP-MS.

Transmission Electron Microscopy (TEM) Imaging of PC-3 Cells and GNRs. PC-3 cells were plated at 50 000 cells/mL in 6-well plates and incubated for 48 h until confluency was reached. The cells were then dosed with both YSA-GNR and Rev-YSA-GNR at a final concentration of 0.1 nM. Cells were then washed, trypsinized, and redispersed in Karnovsky's fixative after 2 and 24 h of incubation time. Cells and GNRs were then centrifuged; the pellet was embedded using osmium tetroxide, potassium ferrocyanide, uranyl acetate, dehydrated with ethanol and acetonitrile, and embedded in an Epon mixture (Lx112 - Ladd, Inc.), polymerized, and sectioned at 60−100 nm using a diamond knife and a Reichart ultramicrotome. Sections were placed on copper grids and stained

with uranyl acetate and lead citrate. Cellular imaging was performed on a Hitachi H600 microscope operating at 75 kV.

AUTHOR INFORMATION

Corresponding Author

*E-mail: murphycj@illinois.edu; Tel.: +1 (217) 333-7680.

Author Contributions

Alaaldin M. Alkilany and Stefano P. Boulos contributed equally to this work.

Notes

The authors declare no competing financial interest.

ACKNOWLEDGMENTS

The authors thank Dr. Sandy McMasters for her assistance with cell cultures, Dr. Alexander Ulanov for his assistance with the GC-MS analysis, Dr. Brian Imai for his assistance with the peptides synthesis, Dr. Rudiger Laufhutte for his assistance with the ICP-MS analysis, Lou Ann Miller for her assistance with Bio-TEM imaging, and Josef Brandauer for helpful discussions. Funding from the National Science Foundation (CHE-1011980) is gratefully acknowledged.

REFERENCES

(1) Dreaden, E. C., Alkilany, A. M., Huang, X., Murphy, C. J., and El-Sayed, M. A. (2012) The golden age: gold nanoparticles for biomedicine. *Chem. Soc. Rev. 41*, 2740−2779.

(2) Mahmoudi, M., Hosseinkhani, H., Hosseinkhani, M., Boutry, S., Simchi, A., Journeay, W. S., Subramani, K., and Laurent, S. (2010) Magnetic resonance imaging tracking of stem cells in vivo using iron oxide nanoparticles as a tool for the advancement of clinical regenerative medicine. *Chem. Rev. 111*, 253−280.

(3) Bardhan, R., Lal, S., Joshi, A., and Halas, N. J. (2011) Theranostic nanoshells: from probe design to imaging and treatment of cancer. *Acc. Chem. Res. 44*, 936−946.

(4) Zhang, Z., Wang, L., Wang, J., Jiang, X., Li, X., Hu, Z., Ji, Y., Wu, X., and Chen, C. (2012) Mesoporous silica-coated gold nanorods as a light-mediated multifunctional theranostic platform for cancer treatment. *Adv. Mater. 24*, 1418−1423.

(5) Kennedy, L. C., Bickford, L. R., Lewinski, N. A., Coughlin, A. J., Hu, Y., Day, E. S., West, J. L., and Drezek, R. A. (2011) A new era for cancer treatment: gold-nanoparticle-mediated thermal therapies. *Small 7*, 169−183.

(6) Schroeder, A., Heller, D. A., Winslow, M. M., Dahlman, J. E., Pratt, G. W., Langer, R., Jacks, T., and Anderson, D. G. (2011) Treating metastatic cancer with nanotechnology. *Nat. Rev. Cancer 12*, 39−50.

(7) Dreaden, E. C., Mackey, M. A., Huang, X., Kang, B., and El-Sayed, M. A. (2011) Beating cancer in multiple ways using nanogold. *Chem. Soc. Rev. 40*, 3391−3404.

(8) Dykman, L., and Khlebtsov, N. (2012) Gold nanoparticles in biomedical applications: recent advances and perspectives. *Chem. Soc. Rev. 41*, 2256−2282.

(9) Alkilany, A. M., Thompson, L. B., Boulos, S. P., Sisco, P. N., and Murphy, C. J. (2012) Gold nanorods: their potential for photothermal therapeutics and drug delivery, tempered by the complexity of their biological interactions. *Adv. Drug Delivery Rev. 64*, 190−199.

(10) Murphy, C. J., Sau, T. K., Gole, A. M., Orendorff, C. J., Gao, J., Gou, L., Hunyadi, S. E., and Li, T. (2005) Anisotropic metal nanoparticles: synthesis, assembly, and optical applications. *J. Phys. Chem. B 109*, 13857−13870.

(11) Huang, X., El-Sayed, I., Qian, W. A., and El-Sayed, M. (2006) Cancer cell imaging and photothermal therapy in the near-infrared region by using gold nanorods. *J. Am. Chem. Soc. 128*, 2115−2120.

(12) Salem, A. K., Searson, P. C., and Leong, K. W. (2003) Multifunctional nanorods for gene delivery. *Nat. Mater. 2*, 668−671.

(13) Wu, G., Mikhailovsky, A., Khant, H. A., Fu, C., Chiu, W., and Zasadzinski, J. A. (2008) Remotely triggered liposome release by near-infrared light absorption via hollow gold nanoshells. *J. Am. Chem. Soc. 130*, 8175−8177.

(14) Wang, L., Liu, Y., Li, W., Jiang, X., Ji, Y., Wu, X., Xu, L., Qiu, Y., Zhao, K., Wei, T., et al. (2011) Selective targeting of gold nanorods at the mitochondria of cancer cells: implications for cancer therapy. *Nano Lett. 11*, 772−780.

(15) Murphy, C. J., Thompson, L. B., Alkilany, A. M., Sisco, P. N., Boulos, S. P., Sivapalan, S. T., Yang, J. A., Chernak, D. J., and Huang, J. (2010) The many faces of gold nanorods. *J. Phys. Chem. Lett. 1*, 2867−2875.

(16) Marega, R., Karmani, L., Flamant, L., Nageswaran, P. G., Valembois, V., Masereel, B., Feron, O., Borght, T. V., Lucas, S., Michiels, C., et al. (2012) Antibody-functionalized polymer-coated gold nanoparticles targeting cancer cells: an in vitro and in vivo study. *J. Mater. Chem. 22*, 21305−21312.

(17) Tkachenko, A. G., Xie, H., Coleman, D., Glomm, W., Ryan, J., Anderson, M. F., Franzen, S., and Feldheim, D. L. (2003) Multifunctional gold nanoparticle−peptide complexes for nuclear targeting. *J. Am. Chem. Soc. 125*, 4700−4701.

(18) Cohen, H., Levy, R. J., Gao, J., Fishbein, I., Kousaev, V., Sosnowski, S., Slomkowski, S., and Golomb, G. (2000) Sustained delivery and expression of DNA encapsulated in polymeric nanoparticles. *Gene Ther. 7*, 1896−1905.

(19) Kim, D., Jeong, Y. Y., and Jon, S. (2010) A drug-loaded aptamer−gold nanoparticle bioconjugate for combined CT imaging and therapy of prostate cancer. *ACS Nano 4*, 3689−3696.

(20) Gobin, A. M., Moon, J. J., and West, J. L. (2008) EphrinA1-targeted nanoshells for photothermal ablation of prostate cancer cells. *Int. J. Nanomed. 3*, 351−358.

(21) Huang, X., Peng, X., Wang, Y., Wang, Y., Shin, D. M., El-Sayed, M. A., and Nie, S. (2010) A reexamination of active and passive tumor targeting by using rod-shaped gold nanocrystals and covalently conjugated peptide ligands. *ACS Nano 4*, 5887−5896.

(22) Koolpe, M., Dail, M., and Pasquale, E. B. (2002) An Ephrin mimetic peptide that selectively targets the EphA2 receptor. *J. Biol. Chem. 277*, 46974−46979.

(23) Wykosky, J., and Debinski, W. (2008) The EphA2 receptor and ephrinA1 ligand in solid tumors: function and therapeutic targeting. *Mol. Cancer Res. 6*, 1795−1806.

(24) Walker-Daniels, J., Coffman, K., Azimi, M., Rhim, J. S., Bostwick, D. G., Snyder, P., Kerns, B. J., Waters, D. J., and Kinch, M. S. (1999) Overexpression of the EphA2 tyrosine kinase in prostate cancer. *Prostate 41*, 275−280.

(25) Blackburn, W. H., Dickerson, E. B., Smith, M. H., McDonald, J. F., and Lyon, L. A. (2009) Peptide-functionalized nanogels for targeted siRNA delivery. *Bioconjugate Chem. 20*, 960−968.

(26) Gole, A., and Murphy, C. J. (2005) Polyelectrolyte-coated gold nanorods: synthesis, characterization and immobilization. *Chem. Mater. 17*, 1325−1330.

(27) Labrador, J. P., Brambilla, R., and Klein, R. (1997) The N-terminal globular domain of Eph receptors is sufficient for ligand binding and receptor signaling. *EMBO J. 16*, 3889−3897.

(28) Holder, N., and Klein, R. (1999) Eph receptors and ephrins: effectors of morphogenesis. *Development 126*, 2033−2044.

(29) Wang, S., Placzek, W. J., Stebbins, J. L., Mitra, S., Noberini, R., Koolpe, M., Zhang, Z., Dahl, R., Pasquale, E. B., and Pellecchia, M. (2012) Novel targeted system to deliver chemotherapeutic drugs to EphA2-expressing cancer cells. *J. Med. Chem. 55*, 2427−2436.

(30) Sano, K., Nakajima, T., Miyazaki, K., Ohuchi, Y., Ikegami, T., Choyke, P. L., and Kobayashi, H. (2013) Short PEG-linkers improve the performance of targeted, activatable monoclonal antibody-indocyanine green optical imaging probes. *Bioconjugate Chem. 24*, 811−816.

(31) Link, S., and El-Sayed, M. A. (1999) Spectral properties and relaxation dynamics of surface plasmon electronic oscillations in gold and silver nanodots and nanorods. *J. Phys. Chem. B 103*, 8410−8426.

(32) Kelly, K. L., Coronado, E., Zhao, L. L., and Schatz, G. C. (2003) The optical properties of metal nanoparticles: the influence of size, shape, and dielectric environment. *J. Phys. Chem. B 107*, 668−677.
(33) Gittins, D. I., and Caruso, F. (2001) Tailoring the polyelectrolyte coating of metal nanoparticles. *J. Phys. Chem. B 105*, 6846−6852.
(34) Masereel, B., Dinguizli, M., Bouzin, C., Moniotte, N., Feron, O., Gallez, B., Vander Borght, T., Michiels, C., and Lucas, S. (2011) Antibody immobilization on gold nanoparticles coated layer-by-layer with polyelectrolytes. *J. Nanopart. Res. 13*, 1573−1580.
(35) Yang, J. A., Lohse, S. E., and Murphy, C. J. (2014) Tuning cellular response to nanoparticles via surface chemistry and aggregation. *Small 10*, 1642−1651.
(36) Malich, G., Markovic, B., and Winder, C. (1997) The sensitivity and specificity of the MTS tetrazolium assay for detecting the in vitro cytotoxicity of 20 chemicals using human cell lines. *Toxicology 124*, 179−192.
(37) Carles-Kinch, K., Kilpatrick, K. E., Stewart, J. C., and Kinch, M. S. (2002) Antibody targeting of the EphA2 tyrosine kinase inhibits malignant cell behavior. *Cancer Res. 62*, 2840−2847.
(38) Alkilany, A., Nagaria, P., Hexel, C., Shaw, T., Murphy, C., and Wyatt, M. (2009) Cellular uptake and cytotoxicity of gold nanorods: molecular origin of cytotoxicity and surface effects. *Small 5*, 701−708.
(39) Dreaden, E. C., Mwakwari, S. C., Sodji, Q. H., Oyelere, A. K., and El-Sayed, M. A. (2009) Tamoxifen−poly(ethylene glycol)−thiol gold nanoparticle conjugates: enhanced potency and selective delivery for breast cancer treatment. *Bioconjugate Chem. 20*, 2247−2253.
(40) Weissleder, R., Kelly, K., Sun, E. Y., Shtatland, T., and Josephson, L. (2005) Cell-specific targeting of nanoparticles by multivalent attachment of small molecules. *Nat. Biotechnol. 23*, 1418−1423.
(41) Bowman, M. C., Ballard, T. E., Ackerson, C. J., Feldheim, D. L., Margolis, D. M., and Melander, C. (2008) Inhibition of HIV fusion with multivalent gold nanoparticles. *J. Am. Chem. Soc. 130*, 6896−6897.
(42) Tassa, C., Duffner, J. L., Lewis, T. A., Weissleder, R., Schreiber, S. L., Koehler, A. N., and Shaw, S. Y. (2010) Binding affinity and kinetic analysis of targeted small molecule-modified nanoparticles. *Bioconjugate Chem. 21*, 14−19.
(43) Conner, S. D., and Schmid, S. L. (2003) Regulated portals of entry into the cell. *Nature 422*, 37−44.
(44) Orendorff, C. J., and Murphy, C. J. (2006) Quantitation of metal content in the silver-assisted growth of gold nanorods. *J. Phys. Chem. B 110*, 3990−3994.
(45) Moore, S., and Stein, W. (1963) Chromatographic determination of amino acids by the use of automatic recording equipment. *Methods Enzymol. 6*, 819−831.
(46) Silva, B. M., Casal, S., Andrade, P. B., Seabra, R. M., Oliveira, M. B., and Ferreria, M. A. (2003) Development and evaluation of a GC/FID method for the analysis of free amino acids in quince fruit and jam. *Anal. Sci. 19*, 1285−1290.
(47) Hušek, P. (1991) Rapid derivatization and gas chromatographic determination of amino acids. *J. Chromatogr. A 552*, 289−299.